



City Research Online

City, University of London Institutional Repository

Citation: Liu, F., Fu, F., Wang, Y. & Liu, Q. (2017). Fire performance of non-load-bearing light-gauge slotted steel stud walls. *Journal of Constructional Steel Research*, 137, pp. 228-241. doi: 10.1016/j.jcsr.2017.06.034

This is the accepted version of the paper.

This version of the publication may differ from the final published version.

Permanent repository link: <https://openaccess.city.ac.uk/id/eprint/17768/>

Link to published version: <https://doi.org/10.1016/j.jcsr.2017.06.034>

Copyright: City Research Online aims to make research outputs of City, University of London available to a wider audience. Copyright and Moral Rights remain with the author(s) and/or copyright holders. URLs from City Research Online may be freely distributed and linked to.

Reuse: Copies of full items can be used for personal research or study, educational, or not-for-profit purposes without prior permission or charge. Provided that the authors, title and full bibliographic details are credited, a hyperlink and/or URL is given for the original metadata page and the content is not changed in any way.

City Research Online:

<http://openaccess.city.ac.uk/>

publications@city.ac.uk

Fire performance of non-load-bearing light-gauge slotted steel stud walls

Faqi Liu^{a,b}, Feng Fu^c, Yuyin Wang^{a,b}, Qiang Liu^{a,b}

(^a Key Lab of Structures Dynamic Behavior and Control (Harbin Institute of Technology), Ministry of Education, Heilongjiang, Harbin, 150090, China;

^b School of Civil Engineering, Harbin Institute of Technology, Heilongjiang, Harbin, 150090, China;

^c School of Mathematics, Computer Science & Engineering, Department of Civil Engineering, City University, London, EC1V 0HB, U.K.)

Abstract

Experimental and numerical studies on the performance of light-gauge slotted steel stud walls subjected to fire are presented in this paper. Four full-scale light-gauge slotted steel stud walls were tested under the ISO-834 standard fire loading. Temperatures at the location of exposed surface, unexposed surface, and cross section of steel studs were measured. Spalling of the heated gypsum board during testing was investigated. The major factors affecting the behavior of this type of wall, including the height of the web, layers of gypsum boards and use of mortar on unexposed surface, were studied.

Based on the test results, a three-dimensional FE model of the light-gauge slotted steel stud wall was developed using ABAQUS to analyze its fire performance. The model was validated against experiments in this study and other related test data. The FE model was employed to conduct further parametric studies. Parameters include the spalling time of heated gypsum boards, the height of the web, rows of slots, and layers of gypsum boards. The effects of these key factors on the temperatures of the exposed surface, unexposed surface and studs are discussed.

Keywords: Experiments, fire performance, light-gauge slotted steel stud wall, numerical study

1 Introduction

Light-gauge steel stud walls are fabricated with thin-walled cold-formed steel stud, gypsum sheathing and insulation materials. These walls possess positive features such as light weight, ease of prefabrication, fast erection, excellent heat insulation and energy efficiency. Therefore in practice this kind of wall has been widely applied as a main load-bearing component in low-rise buildings. However in cold regions, thermal bridging is the main disadvantage of this kind of wall, resulting in problems of condensation and high energy loss in buildings [1].

In order to reduce thermal bridging, the steel webs are slotted to enhance thermal effectiveness. However, the slots in the web reduce the bearing capacity of the wall. If the light-gauge steel stud walls are used as non-load-bearing partition walls, only the self-weight and wind load (for external wall) need to be borne. Therefore more rows of slots can be used and the perforation ratio (ratio of total height of slots and web height) can reach as high as 50%. Slots can also be punched out along the whole length of web in this kind of wall. These improvements can further reduce thermal bridging and increase the insulation performance of this kind of wall. Fire performance of this kind of wall is different from that of conventional steel stud walls due to the difference in temperature development.

Extensive research has been done about the fire resistance of the load-bearing light-gauge steel stud walls. Alfawakhiri et al. [2] summarized experimental and numerical studies on the fire performance of load-bearing light gauge steel frame (LSF) walls. Gerlich et al. [3], Kodur and Sultan [4] and Chen et al. [5] tested load-bearing light gauge steel frame walls exposed to fire. Feng et al. [6] studied the thermal performance of LSF walls subjected to fire both experimentally and numerically. Feng et al. [7] studied in theory the lateral deformation and fire resistance of the LSF walls. Shahbazian and Wang [8] proposed a simple method for calculating the temperatures of the steel studs of the LSF walls exposed to fire. Mahendran et al. [9-12] studied the fire performance of a new kind of LSF wall with an insulation layer placed externally between the plasterboards on both sides of the wall. Mahendran et al.

[13,14] studied non-load-bearing LSF walls subjected to fire. To date, no research has been reported on the fire resistance of non-load-bearing light-gauge slotted steel stud walls. The performance of this type of wall under fire loading would differ from conventional walls due to the existence of slots. Therefore it is essential to study the fire performance of this kind of wall. Experimental research on the fire resistance of light-gauge slotted steel stud partition walls was conducted in this paper. Four full-scale slotted stud walls were tested under ISO-834 standard fire loading [15]. Temperatures of exposed surfaces, unexposed surfaces, positions at the cross section of steel studs were measured. Spalling of the heated gypsum board during testing was investigated. Key factors, including the height of the web, layers of gypsum boards and mortar on unexposed surface, were studied to investigate their influences on temperature distributions of the slotted stud walls.

In addition, a three-dimensional FE model of the slotted stud wall was developed using ABAQUS to analyze its fire performance. The model was validated against experiments in this study and other related test data. The FE model was employed to conduct further parametric studies. Parameters include the spalling time of the heated gypsum board, the height of the web, rows of slots, and layers of gypsum boards. The effects of these key factors on the temperatures of the exposed surface, unexposed surface and studs are discussed.

2 Full scale fire test

Four non-load-bearing light-gauge slotted steel stud wall panels were tested to investigate the fire resistance of this type of member under certain parameters. The parameters investigated are the section depth of the frame members (100mm and 150mm), the gypsum board layers (1 layer and 2 layers) and the mortar layer of the unexposed surface of the wall. The dimensions of each of the wall panels are 1800mm×3000mm, as non-load-bearing walls, stud spacing was 600mm. The web perforation ratio was optimized at 50 % (ratio of total height of slots to web height) and the slots were punched out along the whole length of the stud,

both of which maximize the thermal insulation of the wall. The dimension of the web slots is l_u (length) \times l_v (height) \times d_u (horizontal spacing) \times d_v (vertical spacing) = 70mm \times 3mm \times 20mm \times 9mm (Fig.1).

The specimens were tested according to the specifications of the ISO-834 Standard [15]. The detailed specimen parameters are shown in Table 1. In the table, all of the specimens are numbered in this manner. The first letter G or M stands for gypsum board or mortar, respectively. The second letter S or D stands for a single layer or double layer of 12 mm gypsum board on the exposed side, respectively. The last two digits stand for the height of the stud in mm. For all specimens, a single layer of gypsum board was attached on the unexposed side of the wall. For the specimen MS-100, mortar with a thickness of 10mm was pasted on the unexposed surface of wall.

2.1 Design and fabrication of specimen

As shown in Fig.2, the locations of the thermocouples are same for all the 4 tests. In the tests, thermocouples F/C1-1 to F/C1-5 and F/C2-1 to F/C2-5 in group 1 and 2 respectively are designed to measure thermal bridging between the two sides of the wall. Thermocouples S1-1 to S1-7 and S2-1 to S2-7 in group 1 and 2 respectively are designed to measure the temperature distribution across the stud. Thermocouples F/C3-1 and S3-1 to S3-3 in group 3 are designed to measure the effect of the gypsum board gaps. In addition, thermocouples were also placed at another height, in order to test the temperature variation along the height of the wall (group 4, 5).

2.2 Experimental setup

The test was conducted using the multi-purpose fire furnace in Harbin Institute of Technology, as shown in Fig.3. A detailed introduction of the fire furnace is presented in the paper [16]. The fire temperature was applied in accordance with the ISO-834 standard fire curve [15], as shown in Fig.4. Non-load-bearing walls need to satisfy fire resistant

requirements of integrity and insulation. The experiment was terminated when the maximum temperature of unexposed surface of the wall exceeded 180°C or average temperature exceeded 140°C, or criteria of insulation were exceeded, according to ISO-834 Standard [15].

Therefore the fire resistance could be determined.

2.3 Experimental results and discussions

2.3.1 Experiment observation

In test GS-100, steam was observed coming from the unexposed side of the wall at 9 minutes after ignition. More steam was observed 12 minutes into the test. At 14 minutes, cracks were observed on the exposed surface gypsum board. At 16 minutes, the gypsum board began spalling. At 18 minutes, flame was observed on the exposed surface gypsum board. At 23 minutes, a large part of exposed surface gypsum board was observed spalling off. Buckling of stud was observed at 30 minutes. At 43 minutes, flame was observed coming from the unexposed surface and the test was terminated. Fig.5 shows the different phases of the spalling off of the gypsum board for specimen GS-100.

Fig.6 shows the failure modes of specimen GS-100. Similar phenomena were observed for the other three tests, therefore, the test observations for the other three tests are not introduced here. All tests were stopped when flame spread through cracks in the gypsum boards unexposed to fire, which meant integrity was compromised. The maximum temperature and average temperature of the unexposed surfaces was within limits specified in ISO-834 Standard [15]. The fire resistance and failure criteria of these walls are shown in Table 2. According to the Chinese building code GB50016-2014 [17], the partition wall requires 30 or 60 min of fire resistance, depending on the fire endurance level. According to Approved Document B: Fire safety –Volume 1: Dwellinghouses [18], the partition wall needs to satisfy 30 or 60 min of fire resistance for dwelling houses. Specimen GS-150, GD-100 and MS-100 passed the criteria of 60min's fire resistance, while the specimen GS-100 passed the criteria

of 30min's fire resistance. When the height of the web was increased, a higher fire resistance resulted. Specimen GS-150 (61min) obtained a higher fire resistance than that of specimen GS-100 (43min). Compared to specimen GS-100, the specimens GD-100 and MS-100 possess a much higher fire resistance, which proves that it is effective to add gypsum board to the exposed side or spray mortar on the unexposed side to increase fire resistance.

2.3.2 Results discussions

Fig.7 shows the temperatures at different heights of specimen GS-100. It can be seen that, the temperature is uniform along the height of the specimen. After fall-off of gypsum board on the exposed side, part of stud was exposed to fire directly and then the temperature of stud exceeded to that of gypsum board due to the high thermal conductivity of steel. Fall-off of gypsum board was also observed [9,10] and a rapid temperature rise of stud was induced.

Fig.8, Fig.9 and Fig.10 show the temperature development curves for different specimens at different positions. Fig.8 shows the time-temperature curves of the exposed side of the wall. It can be seen that, for four different specimens, two stages can be observed in rising phases of temperature. First stage is fast temperature rising stage, in this stage, temperatures of exposed surface rose sharply in a short time. Second stage is slow temperature rising stage, the temperature rising rate obviously reduced compared to the first stage. The temperature development resembles that of the ISO-834 standard fire curve (see Fig.4). It is also found that in each specimen, that the five temperature monitoring points correlate to each other in the raising phase, which shows that the thermal bridge of the stud has little effect on the temperature of the exposed surface of the wall.

Fig.9 shows the time-temperature curves of different points of the stud in the wall. It can be seen that the temperature curves for the stud of specimen GS-100, GS-150 and MS-100 are divided into three phases. First stage is initial plateau phase, during which the temperature rise rate is low, due to water evaporation and endothermic migration phenomenon. The

second stage is fast temperature rising stage, because the fall-off of the gypsum board exposes the stud to fire directly. The temperatures tend to be uniform in the third stage, because mineral wool has lost its insulation performance. For specimen GD-100, a double layer of gypsum boards were placed on the exposed side. It took much longer time for the gypsum board to spall off, and then the temperature rise rate of the stud section was delayed.

Fig.10 shows time-temperature curves of the unexposed surface. It can be seen that, for GS-100 and GS-150, overall the fire-temperature curve is divided into four stages. Similarly, the first stage is the initial plateau, the second stage is initial temperature rising stage, the third stage is a plateau stage, during which the temperature rise rate reduced due to internal water evaporation and endothermic migration from gypsum board, and the fourth stage is fast temperature rising stage. For specimen GD-100 and MS-100, fast temperature rising stage is delayed because of the double layer of gypsum boards on the exposed side and sprayed mortar on the unexposed side, respectively.

3 Numerical analysis

A FE model was developed using ABAQUS to perform the numerical analysis of this kind of wall. The details of the numerical model are introduced in this section.

3.1 Thermal properties of materials

The specific heat and thermal conductivity of steel defined in EC3 [19] were adopted to simulate steel under high temperatures, which takes into account the phase change of structural steel at a temperature of 735°C. The specific heat and thermal conductivity of the gypsum board proposed by Feng [6] were adopted, as shown in Table 3 and Table 4, in which the effect of moisture evaporation is considered in the specific heat. The specific heat of the mineral wool is not sensitive to temperature, therefore a constant value of 840 kJ/(kg·°C) was adopted. The conductivity for the mineral wool recommended by Wang [20] was used, which is shown in Table 5.

3.2 Elements and boundary conditions

For the wall without openings for doors or windows, the spacing of the stud is taken as 600mm in the simulation. Due to the fact that the heat transfer of the wall is not uniform in different directions because of the slots in the web, a 3D heat transfer model was built. The gypsum board and mineral wool insulation were modeled with DC3D8 elements and the stud was modeled with DS4 elements (Fig.9). A typical FE model is also shown in Fig.9.

In the simulation, the ISO-834 standard fire curve was adopted. The convective heat transfer coefficient and surface emissivity were taken as $25\text{W/m}^2\cdot^\circ\text{C}$ and 0.7 respectively, based on EC1 [21]. The ambient temperature was taken as 20°C for unexposed surface, with convective heat transfer coefficient and surface emissivity of $10\text{W/m}^2\cdot^\circ\text{C}$ [21] and 0.8 [22,23], respectively.

Cracking and spalling of gypsum board usually occur when it is exposed to fire because of its brittleness, which has been confirmed by test results in this study and related studies [5,9,10]. However, no study has considered this phenomenon in numerical simulation. In this FE model, the elements of gypsum board exposed to fire are deactivated using a model change method at a given time to simulate the fall-off of gypsum board. The time to trigger the disappearance was determined by the time when spalling of the gypsum board starts.

3.3 Verification of numerical program

The proposed model was validated with the test results of this paper, the comparison results of specimen GS-100 are demonstrated in Fig.12, in which the FE model (with) and FE model (without) means fall-off of gypsum board was considered and unconsidered, respectively. It can be found that the fall-off of gypsum board has a significant influence on the temperatures of the stud and unexposed side albeit a insignificant influence on that of the exposed side. Therefore the fall-off of gypsum board needs to be included in the FE model. The modelling results of temperature at unexposed surface and stud are close to the test results when effect

of spalling of gypsum board was considered. However, there are discrepancies for the surface exposed to the fire. The main reason for that is the time for gypsum board starts to spall is difficult to be accurately determined. According to the test observation, the time when spalling of gypsum board happens was 16.7min for GS-100, which was taken in the FE model. The whole gypsum board was deactivated in the model, which differs from the gradual fall-off of gypsum board in the test.

A panel tested by Feng [6] was also used for validation of the FE model, which was fabricated with a lipped channel of 100mm×54mm×15mm×1.2mm, one layer of gypsum board (12.5 mm) on both sides and mineral wool core insulation. The comparisons between FE and test results are shown in Fig.13. It can be seen that a high level of correlation is achieved.

3.4 Parametric analysis

A parametric analysis has been performed using the finite element analysis software ABAQUS. The parameters investigated include the spalling time of the heated gypsum board, the height of the web, rows of slots and layers of gypsum boards.

The temperatures of five key points on the light-gauge slotted steel stud wall, as shown in Fig.14, were selected to discuss the influences of these parameters. The five points are located on the fire exposed surface (1 point), unexposed surface (1 point) and the web of stud (3 points), respectively. In addition, the average temperature at the unexposed surface was also analyzed. The non-load-bearing partition wall subjected to fire may fail due to loss of insulation capacity or integrity. It is difficult to replicate the failure of integrity caused by fall-off of gypsum board in a simulation. Therefore the failure criteria of these walls are dominated by the insulation capacity. In practice, gypsum board on the unexposed side needs to be carefully chosen to avoid premature cracking.

3.4.1 The effect of the spalling of the gypsum board

In the test, spalling was observed for the gypsum board exposed to fire. This will result in an increased rate of temperature rising at the stud section. Therefore, the fall-off of the gypsum board has an obvious effect on the fire resistance performance of light-gauge slotted stud steel walls. Therefore, in the analysis, different spalling times (ST), including 1000 seconds, 1500 seconds, 2000 seconds, 2500 seconds and 3000 seconds respectively were chosen to compare their influence, as shown in Fig.15.

It is noticed that, the earlier the gypsum board starts to fall off, the earlier the temperature starts to increase quickly, for point S-1 to S-3 and C-1. After 60 minutes, the spalling time has an insignificant influence on the temperatures of point S-1 and S-2. The spalling time has an obvious influence on the temperature of the unexposed surface, which means the spalling of the gypsum board would significantly decrease fire resistance.

3.4.2 Effect of the height of the stud

For light-gauge slotted steel stud walls, the heights of studs are varied to meet different architectural requirements. The stud section height was defined as 100mm (5 rows of slots), 150mm (7 rows of slots) and 200mm (9 rows of slots) for the parametric study, all corresponding slot ratios were 50%.

As shown in Fig.16, the stud section height has a slight influence on the temperatures near the exposed surface (e.g. point F-1 and S-1). However the influence increases from the exposed side to the unexposed side, as shown in Fig.16. The temperatures decrease with the increasing stud section height. The fall-off of the gypsum board is not considered, because it is difficult to determine an accurate time.

3.4.3 Effect of rows of slots

The slots of the web will decrease the heat transfer and increase the overall heat insulation capacity of the wall. In order to study the influence of slots in the stud web on the

temperatures, walls with a 100mm height of stud with 0 to 6 rows of slots were analysed, as shown in Fig.17, where the fall-off of the gypsum board was not considered. From Fig.17 a) it can be seen that, the rows of web slots have little effect on the temperature of the exposed side. From Fig.17 b) and c) it is obvious that rows of slots affects the temperature measured on the exposed side of stud (S-1) and the unexposed side of the stud (S-3). The temperature of the exposed side of stud gradually increased in relation to the number of slots, whereas the temperature at the unexposed side was gradually reduced. This indicates that, the slots can increase thermal inertia, enhancing the insulation capacity of the wall. As shown in Fig.17 c), there is no correlation between the temperature of S-2 and the number of slots, this is due to a different heat transfer route caused by the number of slots. From Fig.17 e) it can be seen that, the number of slots has larger effect on the temperature of the unexposed side. However, it is also observed that the temperatures of the two specimens with perforation ratio of 50% ($n=5$) and 60% ($n=6$) are close, which means the effect of rows is insignificant when the perforation ratio is greater than 50%. Therefore it is reasonable to use the 50% perforation ratio. Rows of slots have no obvious influence on the average temperature at the unexposed side of wall, as shown in Fig.17 f).

3.4.4 Effect of the gypsum board layers

In order to enhance the thermal insulation capacity, fire resistance and sound insulation, different gypsum board layers can be attached to this type of wall. In order to investigate the effect of layers of gypsum board on the temperature distribution, different layers placed on the exposed surface and unexposed surface were simulated in the model, and corresponding temperature distributions are shown in Fig.18, in which the fall-off of the gypsum was not considered. As shown in Fig.18, the first digit is the layers of the gypsum board on the exposed side, and the second digit is the layers of the gypsum board on the unexposed side. From Fig.18 a), it can be seen that the temperature at the exposed side is not affected by the

layers of the gypsum boards. From b), c) and d) it can be seen that the temperatures of the stud is affected by the number of the gypsum board layers on the exposed surface. However, the numbers of gypsum board layers **has only a slight influence on the temperature of the exposed surface**. From Fig.18 e) and f), it can be seen that the amount of gypsum board layers and their arrangement can have a great effect on the average temperature of the **exposed surface**. **Generally**, the average temperature **decreases** with the increasing number of layers. When the amount of the layers is the same, **it is more effective to place** more gypsum boards at the fire **exposed** side, which will greatly reduce the temperature of the **unexposed** surface and the overall temperature of the wall.

4 Conclusion

This paper presents a study on the fire resistance of **non-load-bearing** light-gauge slotted steel stud partition walls. 4 full-scale fire tests were performed **to obtain failure modes and temperature distributions of this kind of wall**. In addition, a parametric study was performed **using the finite element analysis software ABAQUS**. It was found that the height of the stud, layers of gypsum boards and number of slots have significant influence on the temperatures **reached during a fire**. The cross-section temperatures decrease with increasing stud section height, layers of gypsum boards and rows of slots. More gypsum boards placed on the fire exposure side will greatly reduce the temperature of the **unexposed** surface and the overall temperature of the wall. The spalling of gypsum board has **an negative** influence on the temperatures of the unexposed side and studs. It is difficult to predict the **point at which the fall-off** of the gypsum boards will start, thus further investigation needs to be **conducted**.

5 Acknowledgement

The research presented in this paper was sponsored by the National Natural Science Foundation (No. 51378152), and China Postdoctoral Science Foundation (No. 2016M591535); their financial support is highly appreciated.

6 Reference

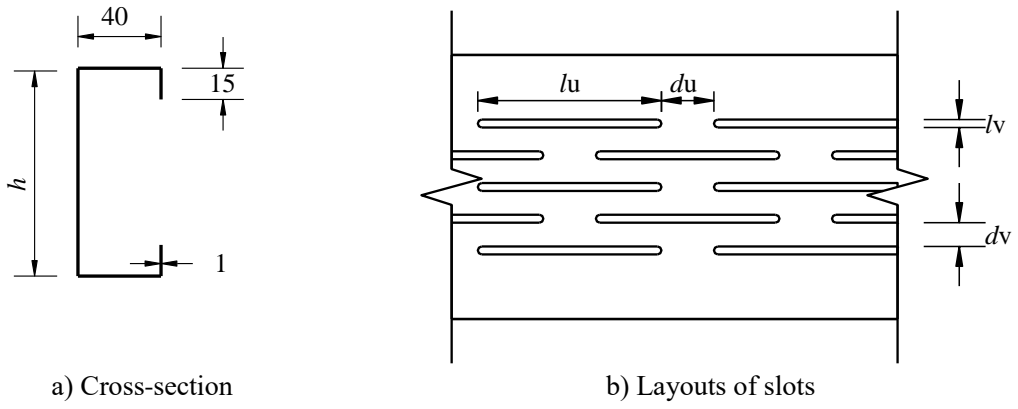
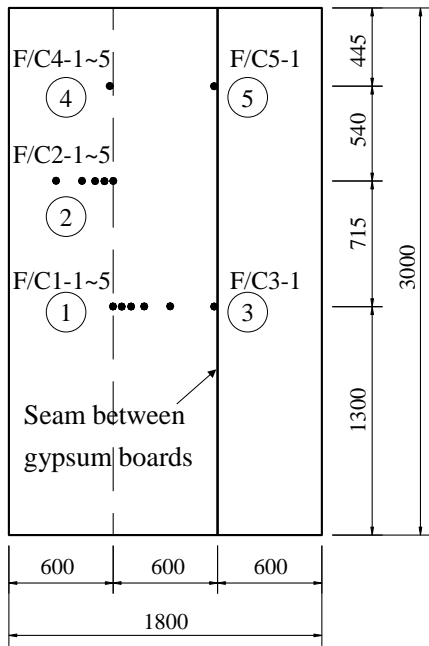
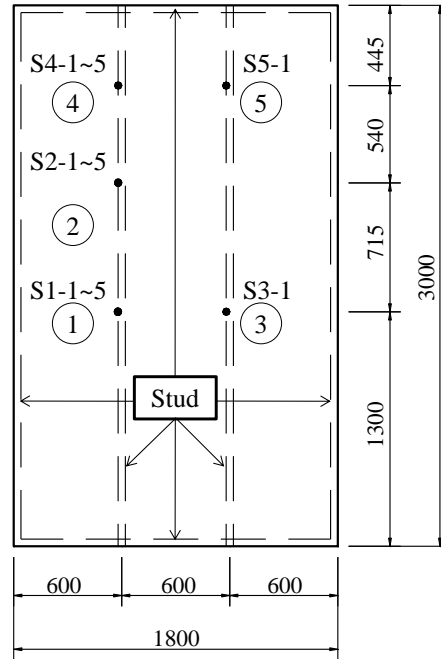


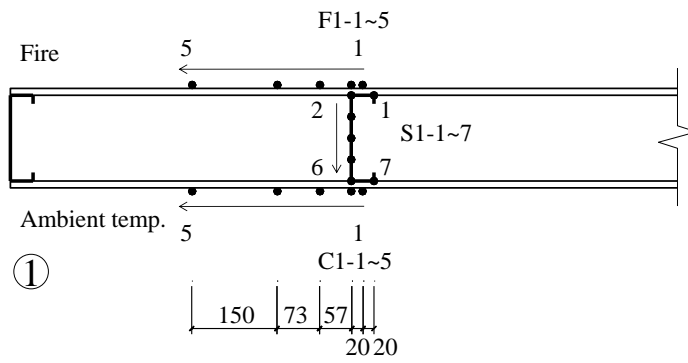
Fig.1 Cross-section of the stud and layouts of slots



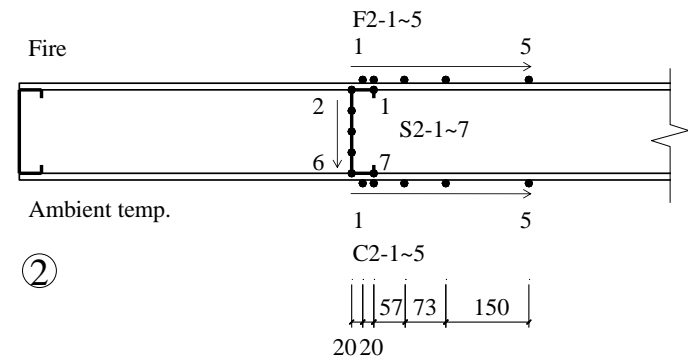
a) Thermocouples on the surface



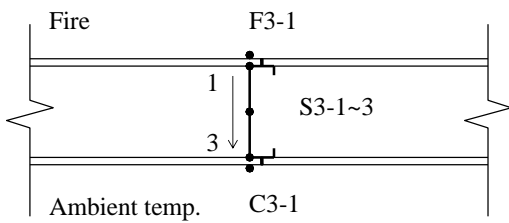
b) Thermocouples on the stud



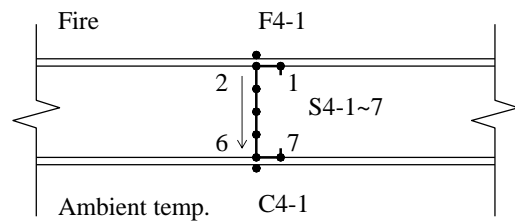
c) Cross section of ①



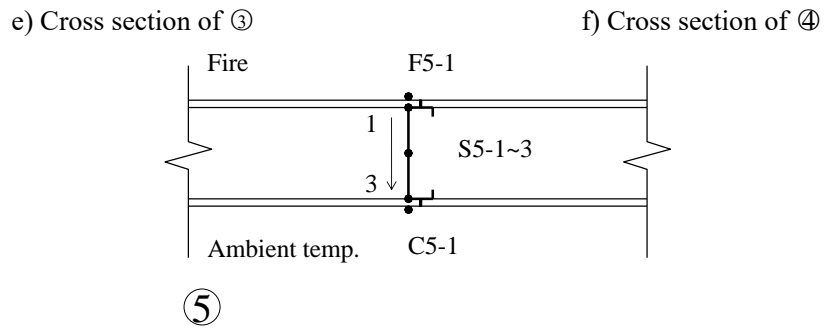
d) Cross section of ②



③



④



g) Cross section of ⑤

Fig. 2 Locations of thermocouples of the wall (unit: mm)



Fig. 3 General view of the test furnace

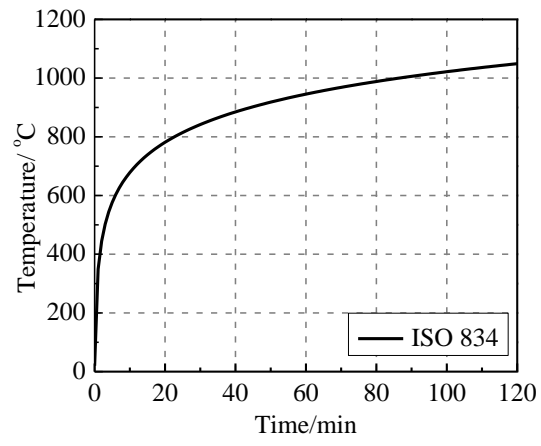


Fig. 4 ISO-834 standard fire temperature curve

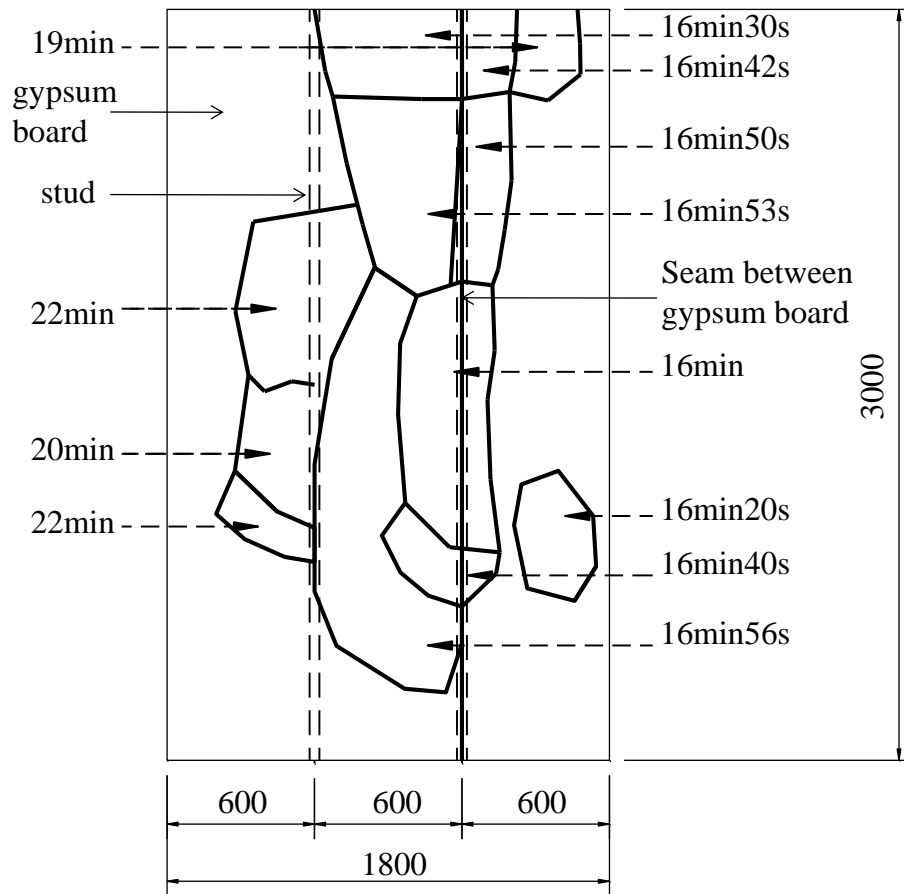


Fig.5 Different phases of the spalling of gypsum board on the exposed side of specimen GS-100 (unit: mm)



a) Exposed surface before test



b) Unexposed surface before test



c) Spalling of the gypsum board on exposed surface



d) Cracking of the gypsum board on unexposed surface

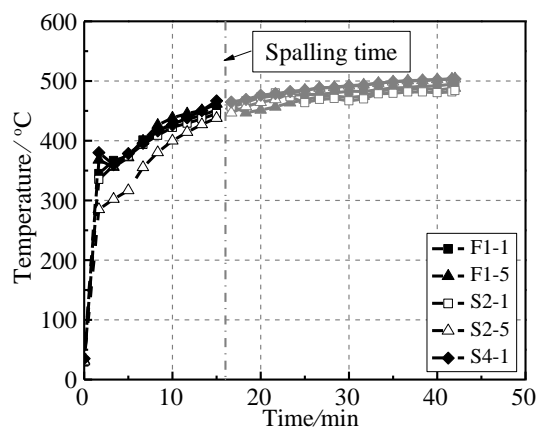


e) Buckling of the stud

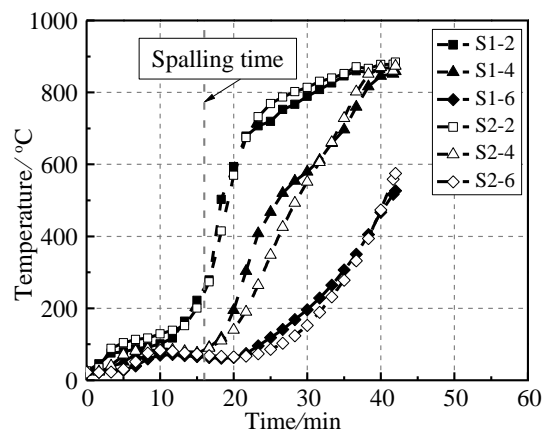


f) Scorching of the mineral wool

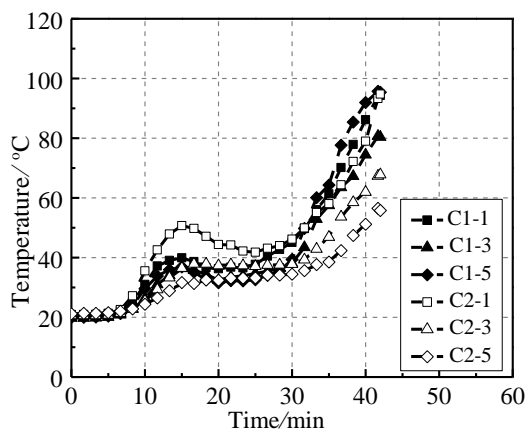
Fig.6 Failure mode of specimen GS-100



a) Exposed surface

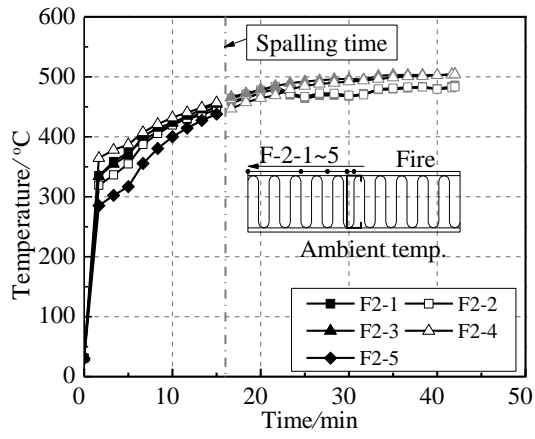


b) Stud

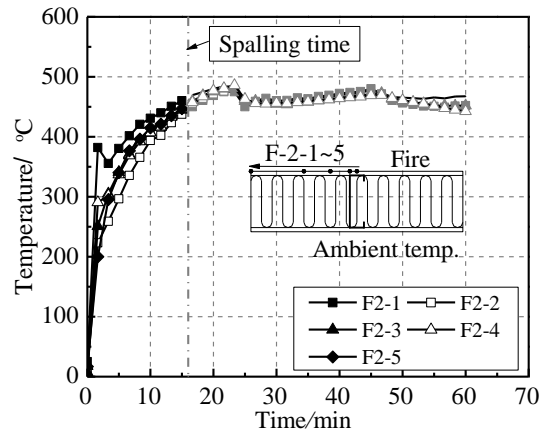


c) Unexposed surface

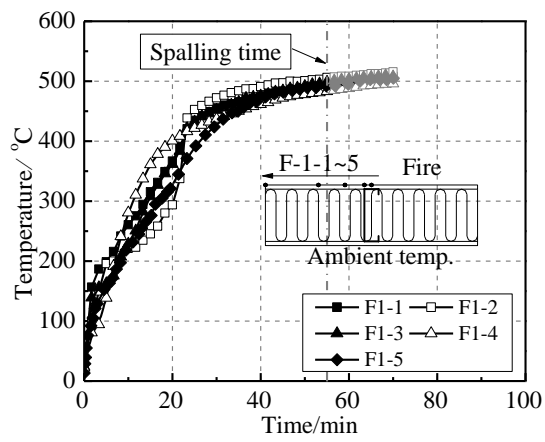
Fig.7 Comparisons of temperatures at different heights of specimen GS-100



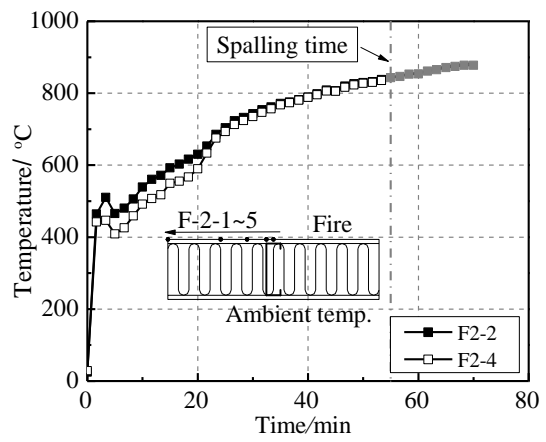
a) GS-100



b) GS-150

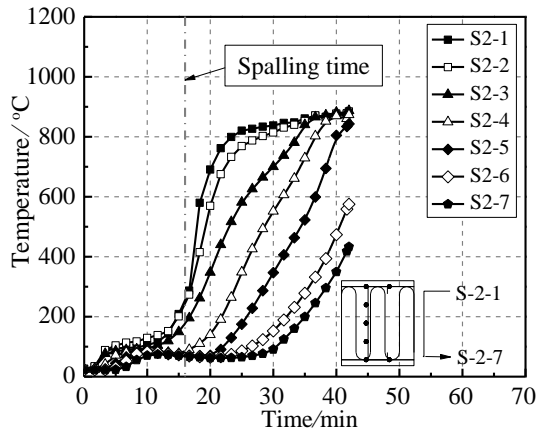


c) GD-100

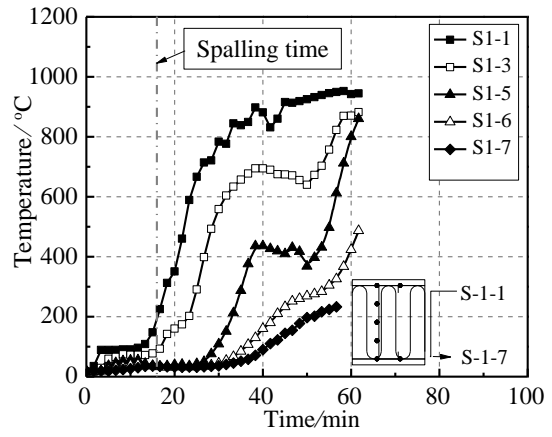


d) 100-MD

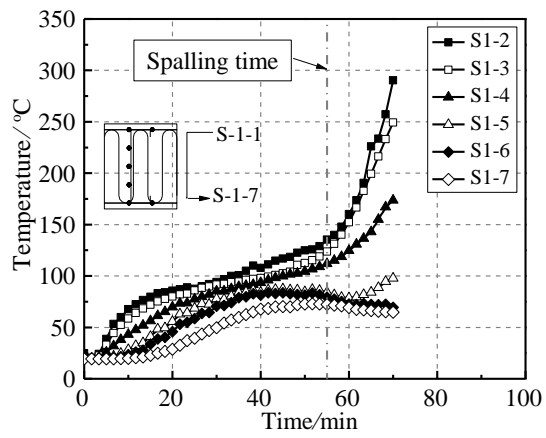
Fig.8 Time-temperature curves of the fire exposed side of the wall



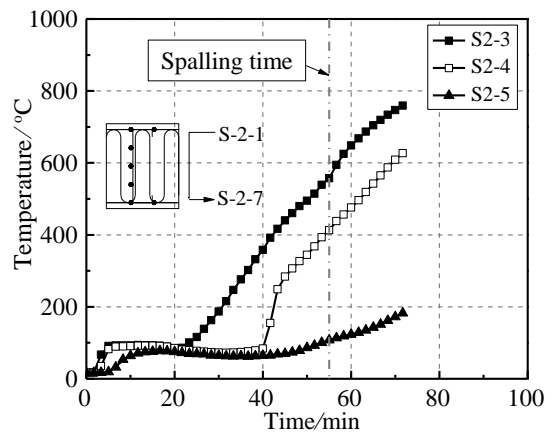
a) GS-100



b) GS-150

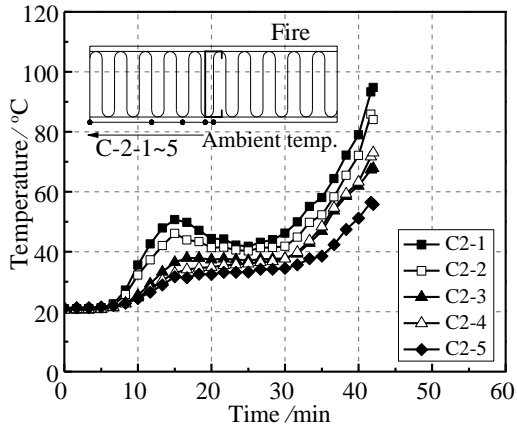


c) GD-100

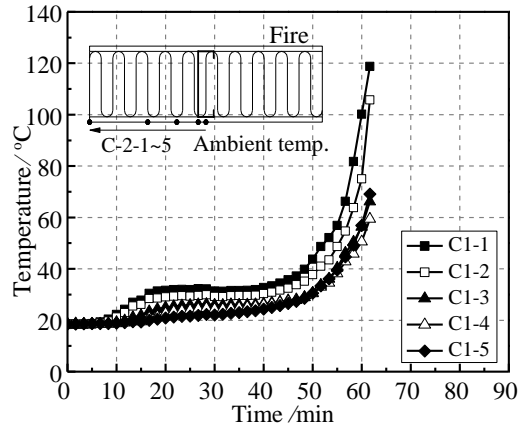


d) MS-100

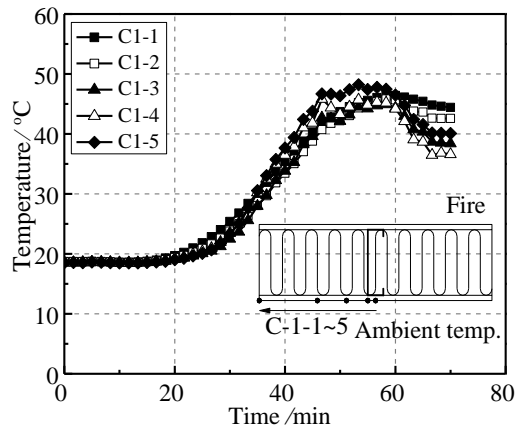
Fig.9 Time-temperature curves of the stud of the wall



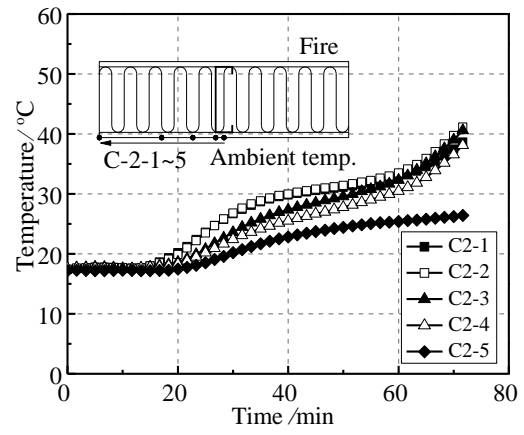
a) GS-100



b) GS-150

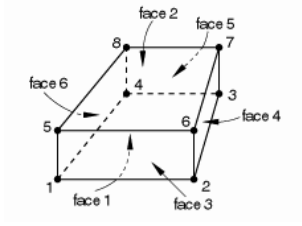


c) GD-100

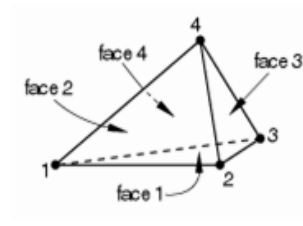


d) MS-100

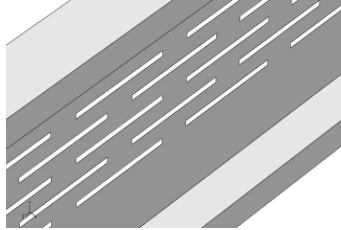
Fig.10 Time-temperature curves of the unexposed surface



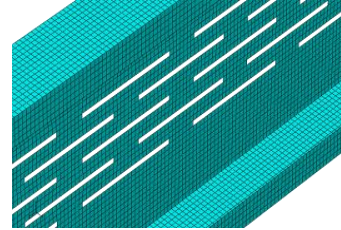
a) DC3D8 element



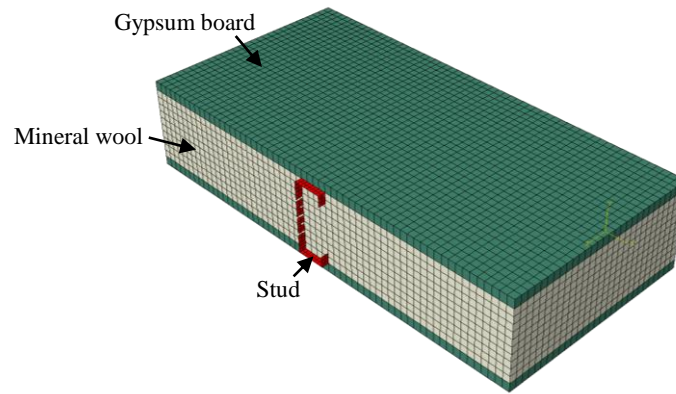
b) DS4 element



c) stud with slots

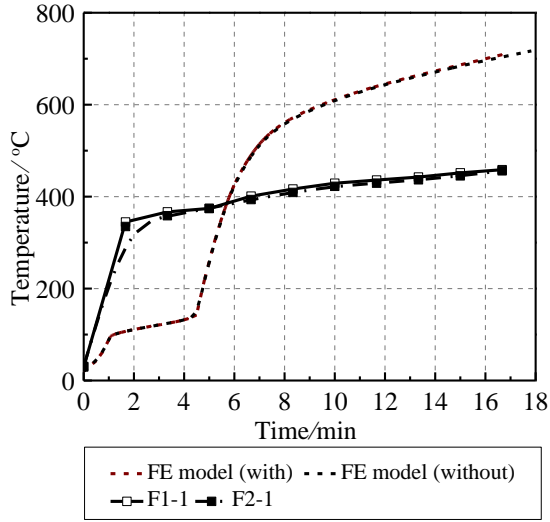


d) Meshes of stud

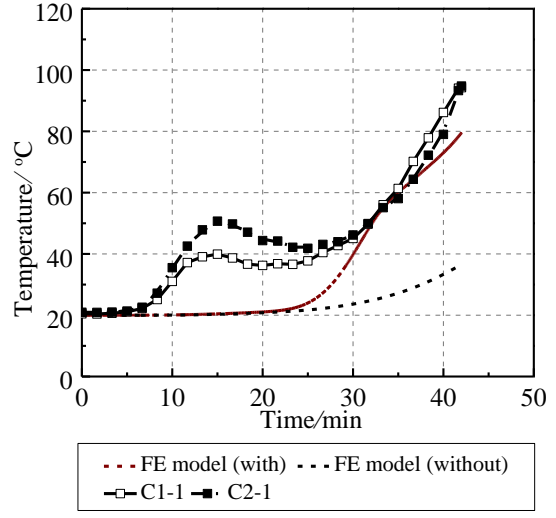


e) FE model

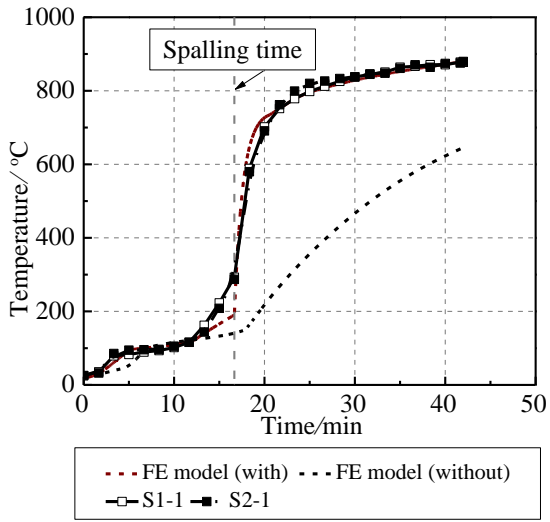
Fig.11 Elements and FE model



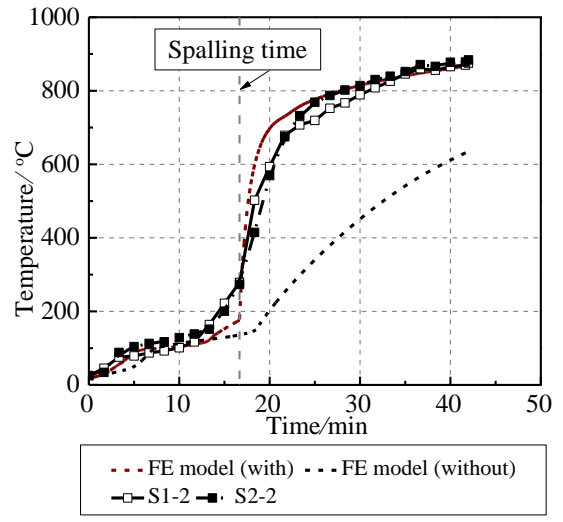
a) Point 1 on exposed surface



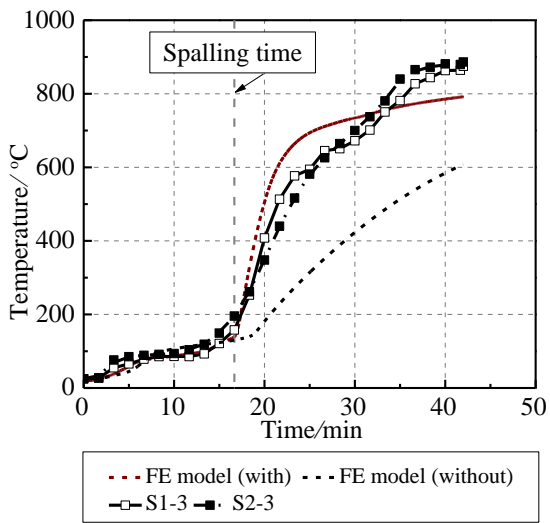
b) Point 1 on unexposed surface



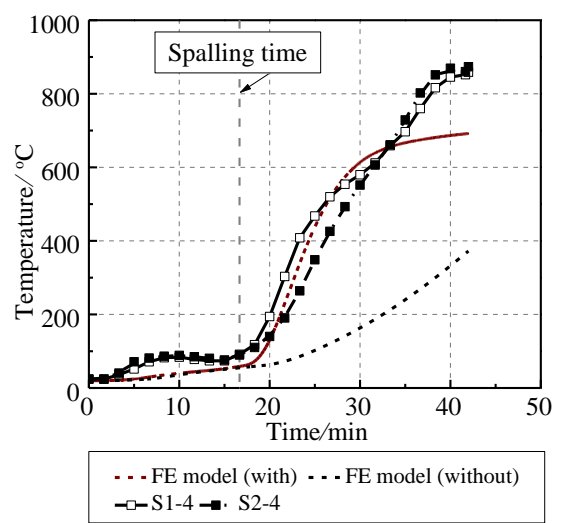
c) Point 1 on stud



d) Point 2 on stud



e) Point 3 on stud



f) Point 4 on stud

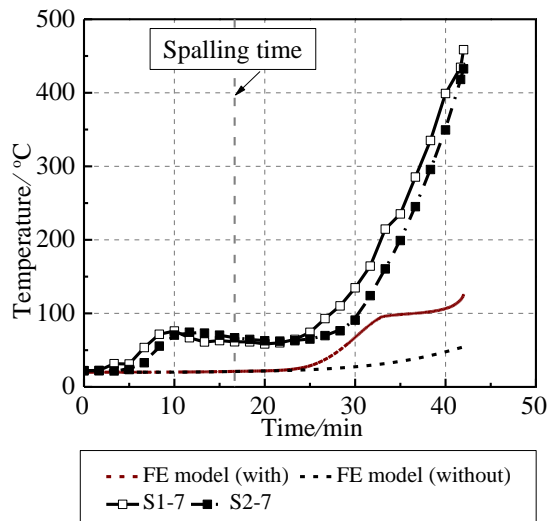
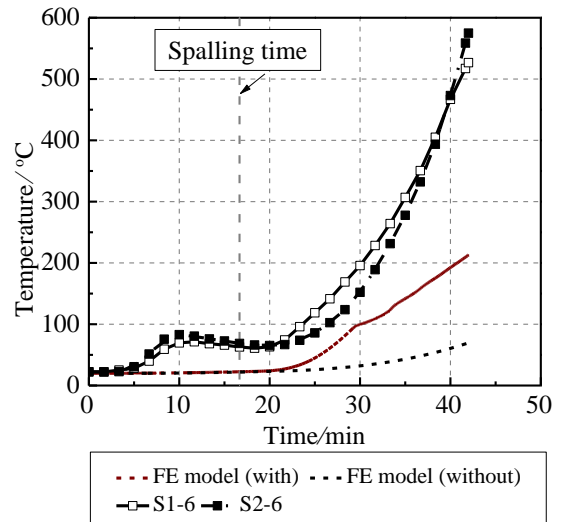
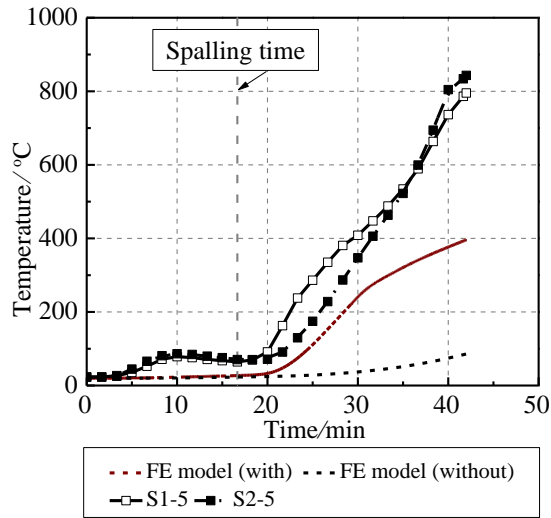
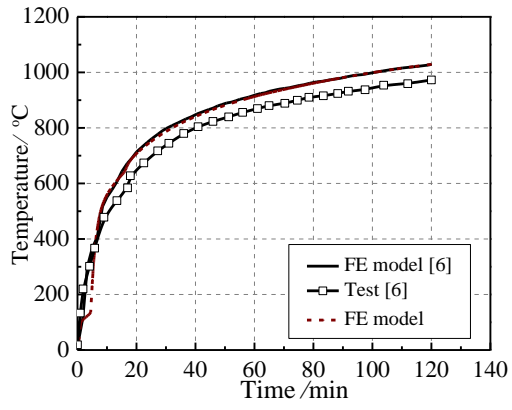
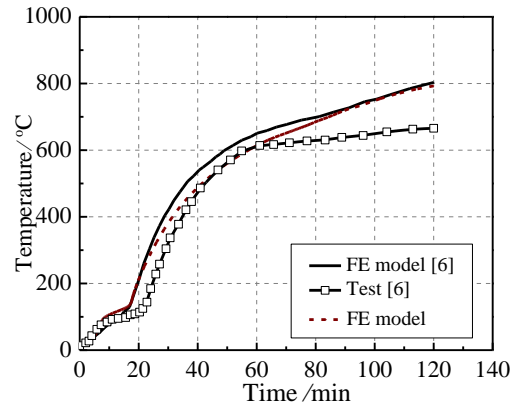


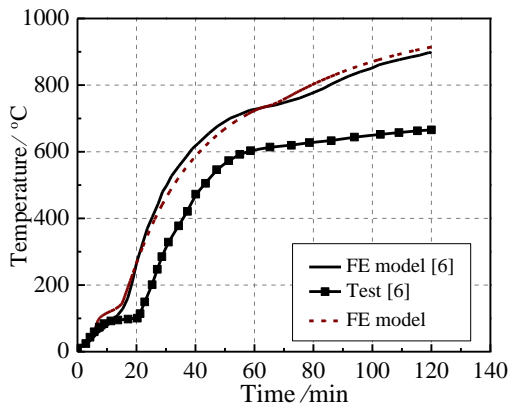
Fig.12 Comparisons between FE and test temperatures(GS-100)



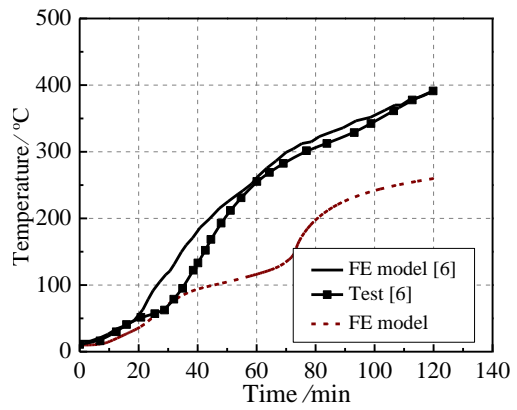
a) Point 1



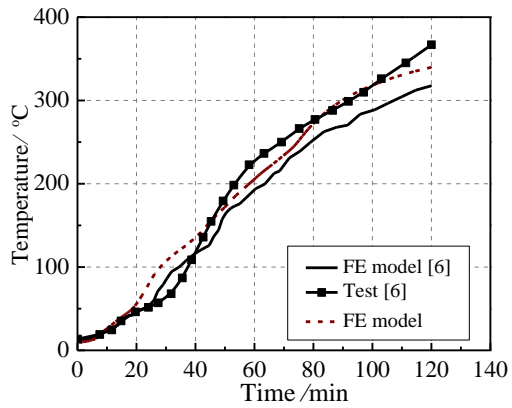
b) Point 2



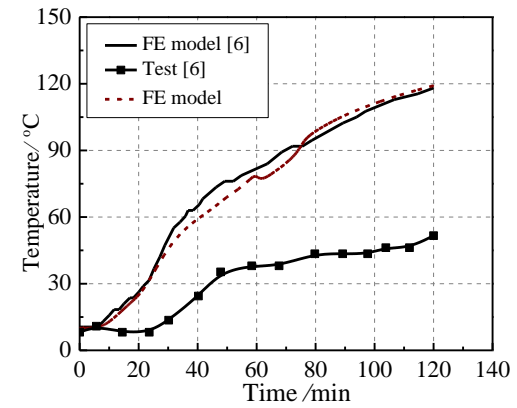
c) Point 3



d) Point 4



e) Point 5



f) Point 6

Fig.13 Validation against test results of Feng [6]

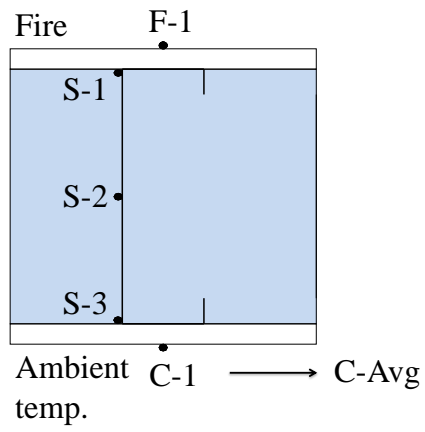
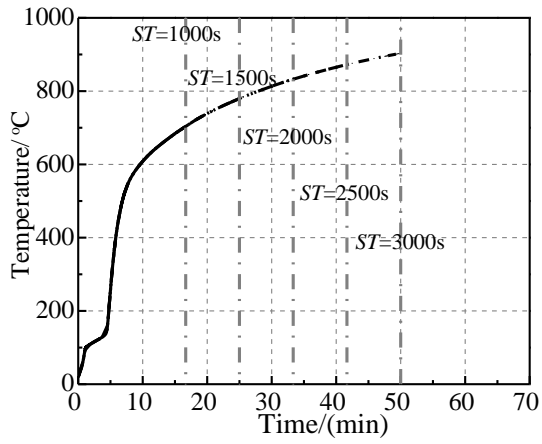
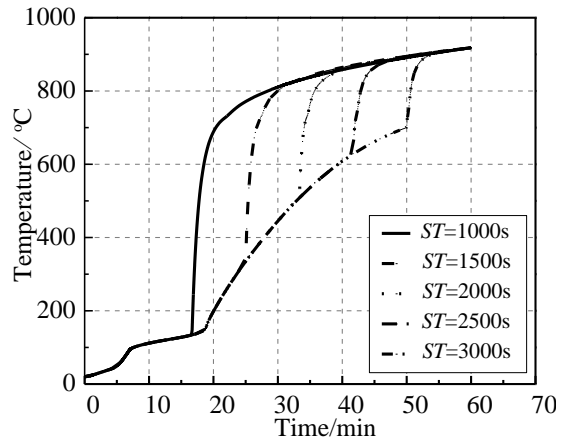


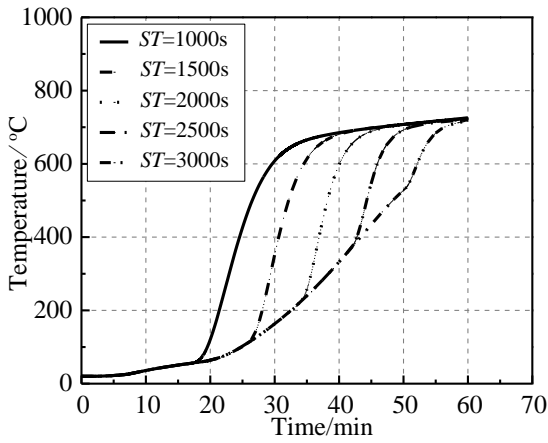
Fig.14 Key points of the cross-section



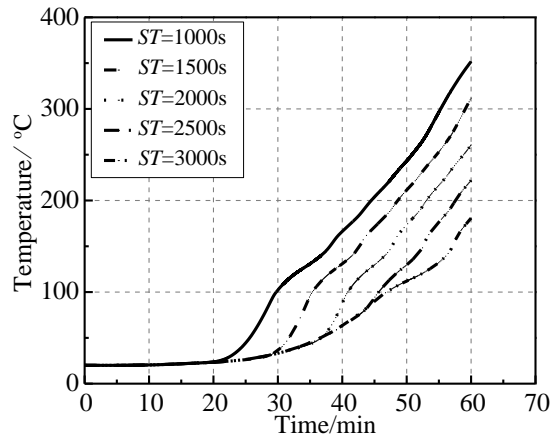
a) Point F-1



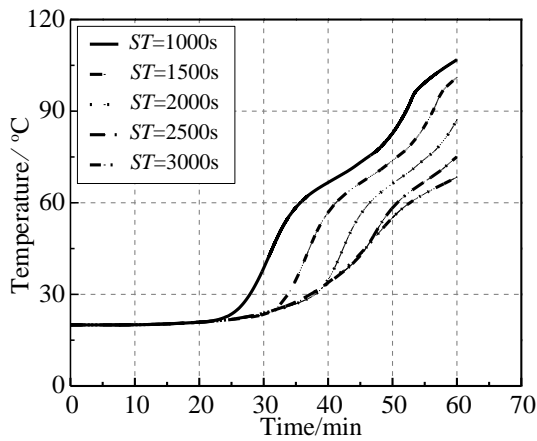
b) Point S-1



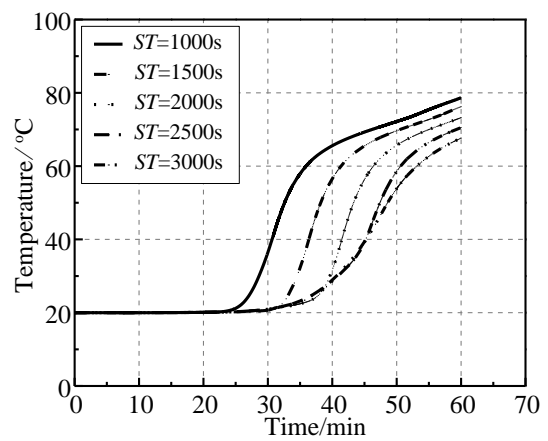
c) Point S-2



d) Point S-3

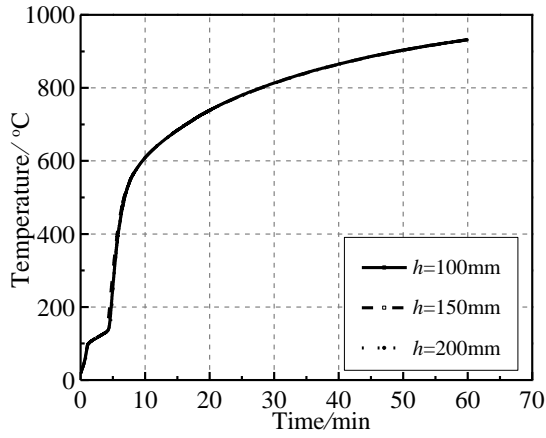


e) Point C-1

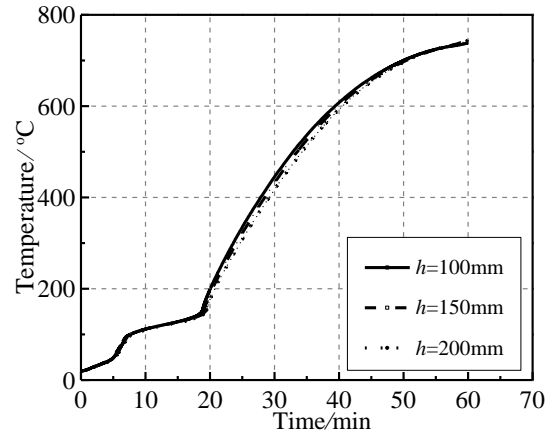


f) Point C-Avg

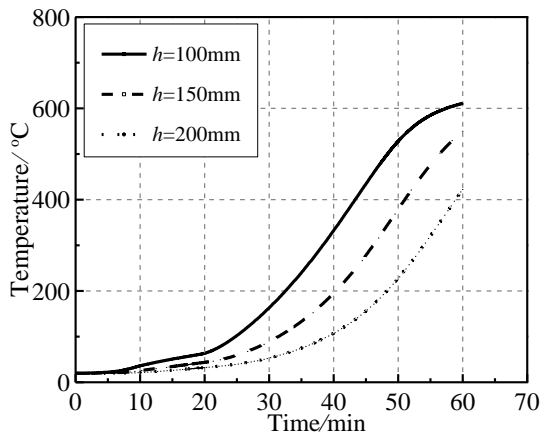
Fig.15 Effect of the spalling time of gypsum board



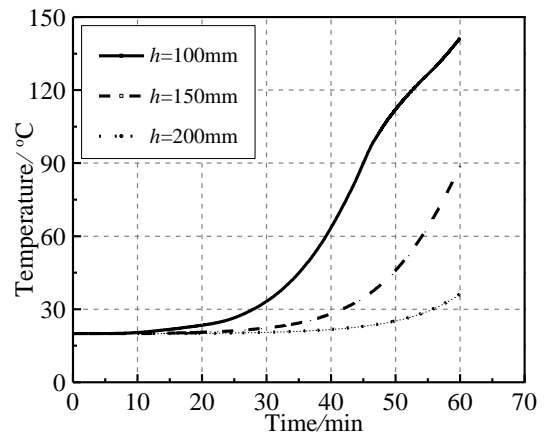
a) Point F-1



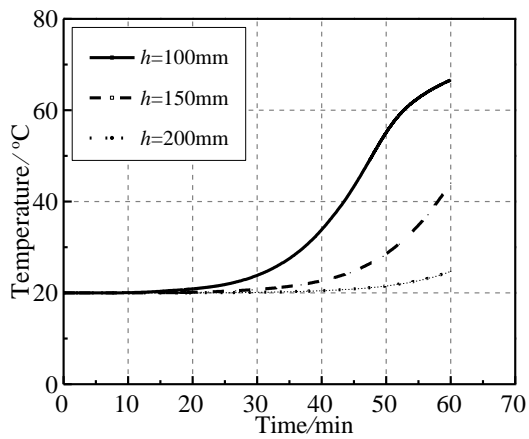
b) Point S-1



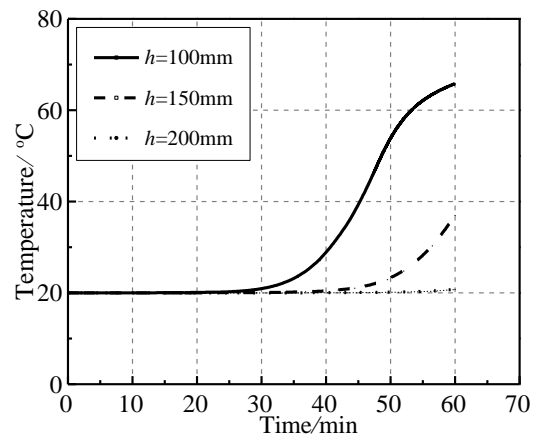
c) Point S-2



d) Point S-3

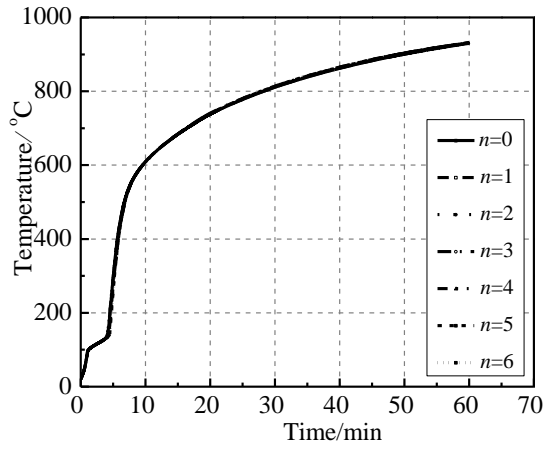


e) Point C-1

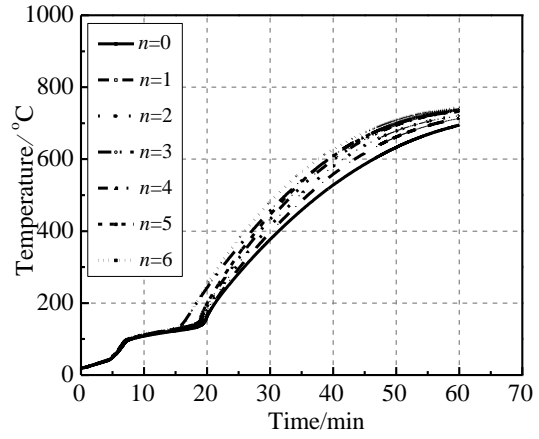


f) Point C-Avg

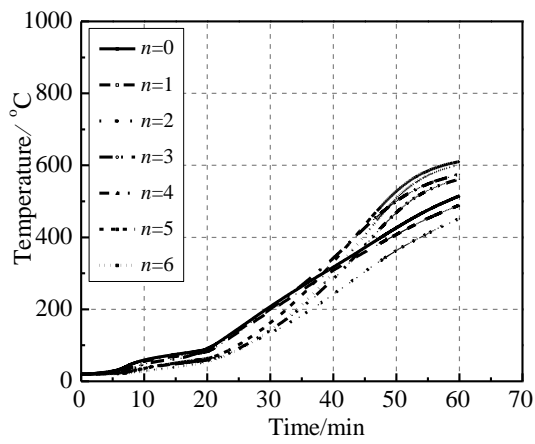
Fig.16 Effect of the height of the web



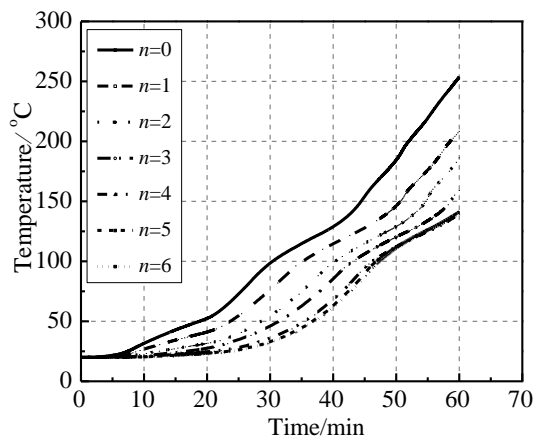
a) Point F-1



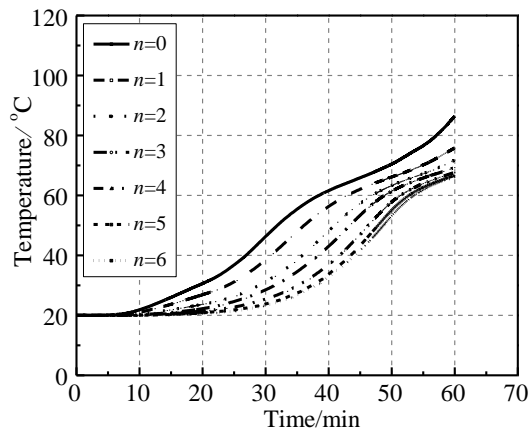
b) Point S-1



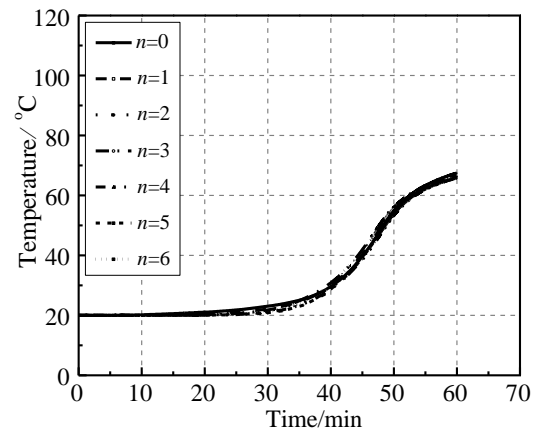
c) Point S-2



d) Point S-3

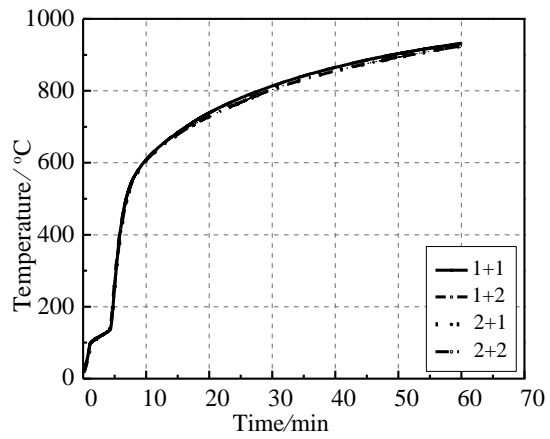


e) Point C-1

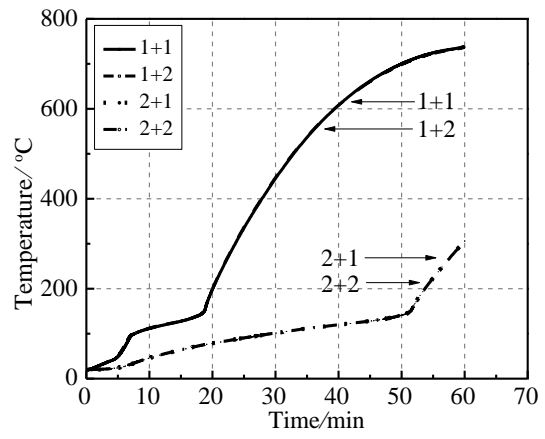


f) Point C-Avg

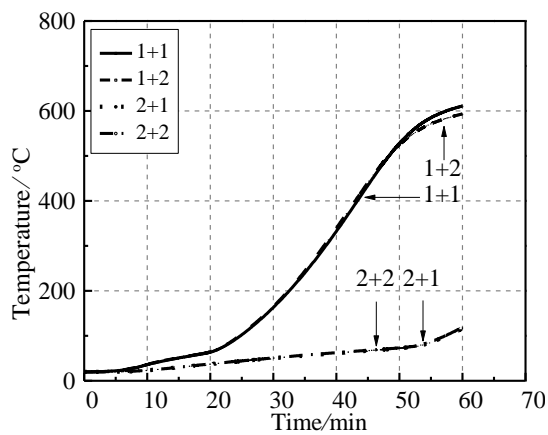
Fig.17 Effect of rows of slots



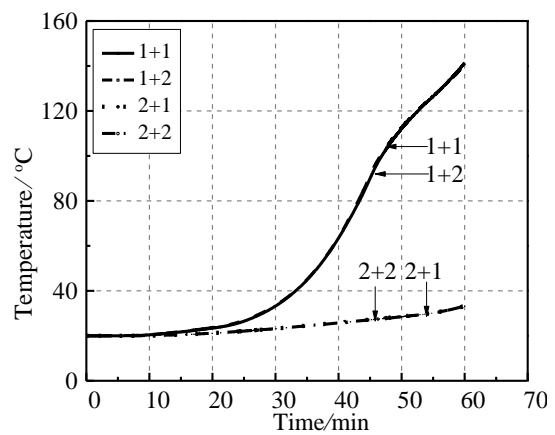
a) Point F-1



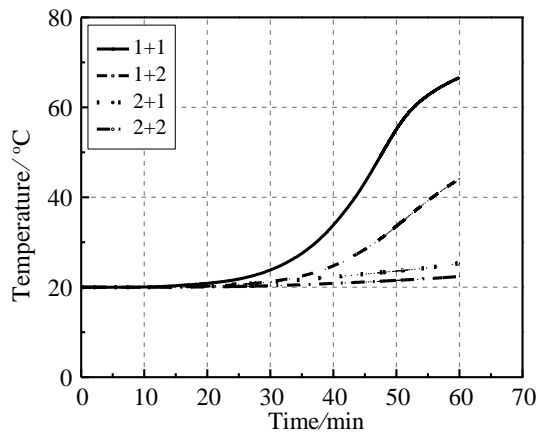
b) Point S-1



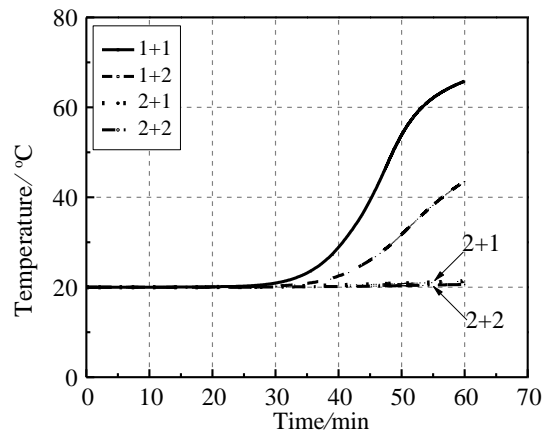
c) Point S-2



d) Point S-3



e) Point C-1



f) Point C-Avg

Fig.18 Effect of layers of gypsum board

Table 1 Details of the specimens

Specimen No.	Rows of slots	Height of Web (mm)	Configurations
GS-100	5	100	<p>12mm gypsum boards Fire Ambient</p>
GS-150	7	150	<p>12mm gypsum boards Fire Ambient</p>
GD-100	5	100	<p>12mm gypsum boards Fire Ambient</p>
MS-100	5	100	<p>12mm gypsum boards Fire Ambient 10mm mortar</p>

Table 2 Fire resistance and failure criteria of the specimens

Specimen No.	Fire resistance (min)	Integrity criteria	Insulation criteria	
			Average temp. (°C)	Maximum temp. (°C)
GS-100	43	Fail	75.1	94.8
GS-150	61	Fail	83.8	118.7
GD-100	70	Fail	40.4	44.4
MS-100	70	Fail	40.0	41.1

Table 3 Specific heat of gypsum board [6]

Temperature (°C)	10	95	125	155	900
Specific heat (kJ/kg·°C)	925.04	941.5	24572.3	953.14	1097.5

Table 4 Thermal conductivity of gypsum board [6]

Temperature (°C)	10	100	150	1200
Thermal conductivity (W/m·°C)	0.26	0.26	0.15	0.3195

Table 5 Thermal conductivity of mineral wool [20]

Temperature (°C)	10	50	150	200	250	300	350	400	450	550	600	650	700	1000
Thermal conductivity (W/m·°C)	0.034	0.037	0.054	0.066	0.08	0.097	0.108	0.113	0.15	0.32	0.52	0.82	1	1.2

- [1] Wang Y C, Salhab B. Structural behaviour and design of lightweight structural panels using perforated cold-formed thin-walled sections under compression. *International Journal of Steel Structures*, 2009, 9(1): 57-67.
- [2] Alfawakhiri F, Sultan M A, MacKinnon D H. Fire resistance of loadbearing steel-stud wall protected with gypsum board: a review. *Fire Technology*, 1999, 35(4): 308-335.
- [3] Gerlich J T, Collier P C R, Buchanan A H. Design of light steel - framed walls for fire resistance. *Fire and Materials*, 1996, 20(2): 79-96.
- [4] Kodur V K R, Sultan M A. Factors influencing fire resistance of load-bearing steel stud walls. *Fire technology*, 2006, 42(1): 5-26
- [5] Chen W, Ye J, Bai Y, Zhao X L. Full-scale fire experiments on load-bearing cold-formed steel walls lined with different panels. *Journal of Constructional Steel Research*, 2012, 79: 242-254.
- [6] Feng M, Wang Y C, Davies J M. Thermal performance of cold-formed thin-walled steel panel systems in fire. *Fire safety journal*, 2003, 38(4): 365-394.
- [7] Feng M, Wang Y C. An analysis of the structural behaviour of axially loaded full-scale cold-formed thin-walled steel structural panels tested under fire conditions. *Thin-walled structures*, 2005, 43(2): 291-332.
- [8] Shahbazian A, Wang Y C. A simplified approach for calculating temperatures in axially loaded cold-formed thin-walled steel studs in wall panel assemblies exposed to fire from one side. *Thin-Walled Structures*, 2013, 64: 60-72.
- [9] Gunalan S, Kolarkar P, Mahendran M. Experimental study of load bearing cold-formed steel wall systems under fire conditions. *Thin-Walled Structures*, 2013, 65: 72-92.
- [10] Ariyanayagam A, Mahendran M. Experimental study of load-bearing cold-formed steel walls exposed to realistic design fires. *Journal of Structural Fire Engineering*, 2014,

5(4): 291-330.

- [11] Gunalan S, Mahendran M. Finite element modelling of load bearing cold-formed steel wall systems under fire conditions. *Engineering Structures*, 2013, 56: 1007-1027.
- [12] Ariyanayagam A D, Mahendran M. Fire design rules for load bearing cold-formed steel frame walls exposed to realistic design fire curves. *Fire Safety Journal*, 2015, 77: 1-20.
- [13] Ariyanayagam A D, Mahendran M. Fire tests of non-load bearing light gauge steel frame walls lined with calcium silicate boards and gypsum plasterboards. *Thin-Walled Structures*, 2017, 115: 86-99.
- [14] Keerthan P, Mahendran M. Numerical modelling of non-load-bearing light gauge cold-formed steel frame walls under fire conditions. *Journal of Fire Sciences*, 2012, 30(5): 375-403.
- [15] ISO-834. Fire resistance tests - elements of building construction. Switzerland: International Organization for Standardization; 1999.
- [16] Liu F, Gardner L, Yang H. Post-fire behaviour of reinforced concrete stub columns confined by circular steel tubes. *Journal of Constructional Steel Research*, 2014, 102: 82-103.
- [17] GB50016. Code for fire protection design of buildings. Beijing: Chinese Code, 2014.
- [18] Approved Document B: Fire safety –Volume 1: Dwellinghouses. London, 2007.
- [19] CEN. Eurocode 3: design of steel structures - Part 1-2: general rules - structural fire design. EN1993-1-2:2005. Brussels: European Standard, 2005.
- [20] Wang H B. Heat transfer analysis of components of construction exposed to fire-a theoretical, numerical and experimental approach. Diss. PhD thesis, Civil Engineering and Construction, University of Salford, 1995.
- [21] CEN. Eurocode 1: actions on structures - Part 1-2: general actions - actions on structures exposed to fire. EN1991-1-2:2002. Brussels: European Standard, 2002.
- [22] Rahmanian I, Wang Y C. A combined experimental and numerical method for extracting temperature-dependent thermal conductivity of gypsum boards. *Construction and Building Materials*, 2012, 26(1): 707-722.
- [23] Weber B. Heat transfer mechanisms and models for a gypsum board exposed to fire. *International Journal of Heat and Mass Transfer*, 2012, 55(5): 1661-1678.